Raport Badawczy

Research Report

RB/61/2003

Designing PI controllers for robust stability and performance

W. Krajewski

Instytut Badań Systemowych
Polska Akademia Nauk

Systems Research Institute
Polish Academy of Sciences

POLSKA AKADEMIA NAUK

Instytut Badań Systemowych

ul. Newelska 6

01-447 Warszawa

tel.: (+48) (22) 8373578

fax: (+48) (22) 8372772

Kierownik Pracowni zgłaszający pracę:
Prof. dr hab. Krzysztof C. Kiwiel

Warszawa 2003

Designing PI Controllers for Robust Stability and Performance

Wieslaw Krajewski, Antonio Lepschy and Umberto Viaro

Abstract

The design of PI controllers can profitably be carried out by referring to a normalized process model and to the loci of constant stability margins and cross-over frequency in the parameter space. These loci are easily obtained from linear interpolation conditions. After checking the compatibility of the specifications with the controller structure, it is shown how the above-mentioned loci can be exploited for tuning purposes and robustness analysis. Criteria for choosing the controller parameters within the admissible region are discussed with the aid of examples.

Index Terms — **PI controllers, first-order lag plus dead-time process models, stability margins, parameter-plane stability regions.**

I. INTRODUCTION

When dealing with PID control, it is customary to recall that: (*i*) according to surveys on the state of process control systems, more than 90% of the control loops are of the PID type [1], most of which use PI control only (97% in the pulp and paper industry [2]), and large part of them are poorly tuned [3]; (*ii*) an important reason of the continual interest in such kind of controllers is the spreading of centralized computer control systems; (*iii*) in the majority of industrial applications, a simple first-order-lag-plus-delay (FOLPD) model of the plant proves adequate [4] for design and tuning since the seminal paper by Ziegler and Nichols [5]. In view of these facts, it is not surprising that many recent research papers are devoted to the subject (cf., e.g., [6]-[10]).

Clearly, the FOLPD model can only be an approximation of the actual plant behavior so that robustness issues play a major role. Traditionally, stability margins have been used as meaningful measures of robustness with respect to both system stability and performance, and PID design techniques have been developed to satisfy gain and phase margin specifications, possibly in conjuction with performance optimization criteria. In particular, in [11] the transcendental equations expressing magnitude and phase of the loop frequency response have been solved numerically for the cross-over frequencies and controller parameters, and the ISE for various combinations of stability margins have been computed to allow a tradeoff between these margins and performance.

Now, the phase margin m_ϕ accounts well for dynamic precision, especially for the step response overshoot, but is not related to its rise time which depends instead on the gain cross-over frequency ω_A. On the other hand, the requirement of steady-state accuracy is satisfied by the presence of the integral action in both PI and PID controllers; therefore it is reasonable to first check whether a PI controller is enough, and resort to a PID controller otherwise. For these reasons, the paper refers to specifications regarding m_ϕ and ω_A and to the PI structure which affords two design parameters and allows us to meet, in many cases, both specifications. In the following sections, simple rules will be provided to ascertain the compatibility of the two specifications with the controller structure.

As will be shown, the suggested method can be extended to the case in which the specifications are given in terms of phase margin m_ϕ and gain margin m_g. However, this criterion seems to be less justified because, with the considered process and PI controller, the magnitude of the open-loop frequency response is monotonically decreasing, which implies that there is a unique intersection of the open-loop Nyquist diagram with the unit circle (for $\omega = \omega_A$). It follows that, very often, if m_ϕ is acceptable, m_g will be sufficiently large too.

This paper is organized as follows. After introducing the essential notation, a simple variable transformation is adopted in Section II leading to a normalized process transfer function characterized by a single parameter. The basic interpolation equations are derived in Section III; they turn out to be linear in the design parameters. Section IV analyses the stability of the feedback control system by determining the stability regions as well as the loci of constant m_ϕ in the parameter space, whereas the loci of constant ω_A are determined in Section V. The possibility of satisfying the specifications with a PI controller is investigated in Section VI by exploiting the loci previously derived. Section VII shows how to avail ourselves of these loci to design the controller and to evaluate the robustness of the resulting

W. Krajewski is with the Systems Research Institute, Polisch Academy of Sciences, ul. Newelska 6, 01 447 Warsaw, Poland (email: krajewsk@ibspan.waw.pl)

A. Lepschy is with the Department of Information Engineering, University of Padova, via Gradenigo 6/A, 35131 Padova, Italy (email: lepschy@dei.unipd.it)

U. Viaro is with the Department of Electrical, Managerial and Mechanical Engineering, University of Udine, via delle Scienze 208, 33100 Udine, Italy (email: viaro@uniud.it)

control system. In Section VIII a similar approach is used to take account of the gain margin. The paper ends with some examples that clearly show how too large phase margins give rise to unacceptable settling times.

Probably the main contributions of the present work are: (*i*) the determination of the loci of constant stability margins and cross-over frequency in the parameter space, and (*ii*) the suggestion of criteria for robust controller tuning based on such loci.

II. MODEL NORMALIZATION

In the following, reference will be made to processes that can adequately be modelled by a transfer function of the form:

$$\hat{P}(\hat{s}) = K\frac{e^{-L\hat{s}}}{1+T\hat{s}},\ K,T,L>0 \tag{1}$$

where the independent variable is denoted by $\hat{s}$ because the symbol s will be used to indicate a normalized variable.

The transfer function of the adopted PI controller is:

$$\hat{C}(\hat{s}) = K_P + \frac{K_I}{\hat{s}} = \frac{K_I}{\hat{s}}(1+T_I\hat{s}) = K_P(1+\frac{1}{T_I\hat{s}}) \tag{2}$$

with

$$T_I = \frac{K_P}{K_I}. \tag{3}$$

Therefore, the open-loop transfer function becomes:

$$\hat{G}(\hat{s}) = \frac{K(K_I+K_P\hat{s})}{\hat{s}}\ \frac{e^{-L\hat{s}}}{1+T\hat{s}}. \tag{4}$$

For the reasons explained in the Introduction, we initially consider specifications in terms of phase margin m_ϕ and gain cross-over frequency $\hat{\omega}_A$.

For normalization purposes, the independent variable will be transformed to:

$$s := T\hat{s} \tag{5}$$

so that (4) becomes:

$$G(s) := \hat{G}(\frac{s}{T}) = \frac{(a+bs)}{s}\ \frac{e^{-\tau s}}{1+s}. \tag{6}$$

where:

$$a := KK_IT, \tag{7a}$$

$$b := KK_P, \tag{7b}$$

$$\tau := \frac{L}{T}. \tag{7c}$$

Accordingly, the specification on $\hat{\omega}_A$ is translated into a constraint on the normalized cross-over frequency:

$$\omega_A := T\hat{\omega}_A, \tag{8}$$

whereas the specification on m_ϕ is not affected by (5).

III. INTERPOLATION CONDITIONS

It is easy to relate the values of parameters a and b to the values of ω_A and m_ϕ, given the value of τ (which is the unique parameter characterizing the process in the normalized transfer function function (6)). Once a and b have been determined, the controller parameters K_P and K_I, or K_P and T_I, can be obtained from (7*a*), (7*b*) and (7*c*).

Necessary conditions for $G(j\omega)$ to exhibit phase $m_\phi - \pi$ (and, thus, for the system to exhibit phase margin m_ϕ) and unit magnitude at ω_A follow immediately from the interpolation condition:

$$G(j\omega_A) = e^{j(m_\phi-\pi)} = -\cos m_\phi - j\sin m_\phi. \tag{9}$$

Multiplying (9) by $j\omega_A - \omega_A^2$, for ω_A real and strictly positive we get:

$$a\cos(\tau\omega_A) + b\omega_A\sin(\tau\omega_A) = \omega_A^2\cos m_\phi + \omega_A\sin m_\phi, \tag{10a}$$

$$-a\sin(\tau\omega_A) + b\,\omega_A\cos(\tau\omega_A) = -\omega_A\cos m_\phi + \omega_A^2\sin m_\phi. \tag{10b}$$

A useful feature of equations (10a), (10b) is their linearity with respect to a and b, which allows us to easily find their unique solution:

$$a = \omega_A[\sin(\tau\omega_A + m_\phi) + \omega_A\cos(\tau\omega_A + m_\phi)], \tag{11a}$$

$$b = \omega_A\sin(\tau\omega_A + m_\phi) - \cos(\tau\omega_A + m_\phi). \tag{11b}$$

Clearly, conditions (10a), (10b) are not sufficient to achieve the desired stability margin m_ϕ because, even if the Nyquist diagram of $G(j\omega)$ passes through point $e^{j(m_\phi-\pi)}$, it could encircle point $-1+j0$ (see Section IV).

In the following sections, the above equations will be exploited to check the compatibility of the considered specifications, to design the controller and to evaluate the system robustness.

IV. STABILITY ANALYSIS

The Nyquist diagram of the type-one loop function $G(j\omega)$ for $\omega \longrightarrow 0_+$ tends to a vertical asymptote whose abscissa is:

$$r := \lim_{\omega\to 0} Re[G(j\omega)] = b - (1+\tau)a. \tag{12}$$

Moreover we have:

$$sgn\{\lim_{\omega\to 0_+} Im[G(j\omega)]\} = -sgn\,a. \tag{13}$$

It follows that the initial arc (ω small) of the (positive) Nyquist diagram belongs to:

(i) the first quadrant for $a<0$, $b>(1+\tau)a$;
(ii) the second quadrant for $a<0$, $b<(1+\tau)a$;
(iii) the third quadrant for $a>0$, $b<(1+\tau)a$;
(iv) the fourth quadrant for $a>0$, $b>(1+\tau)a$.

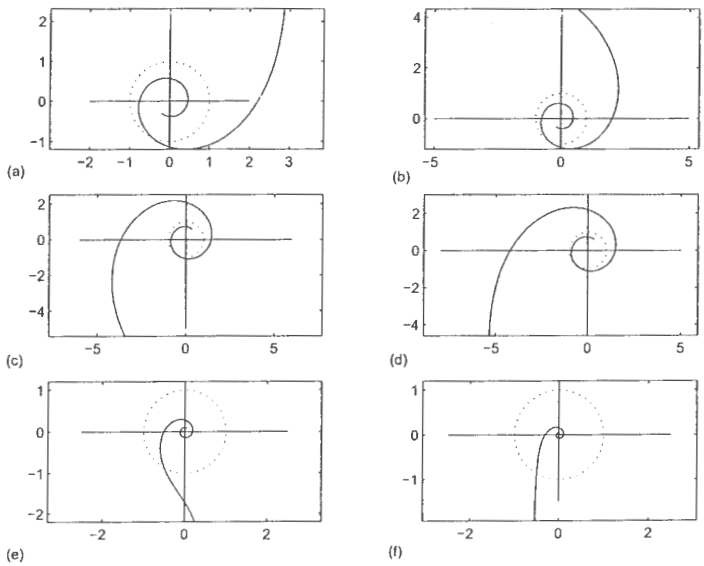

Fig. 1. Typical Nyquist diagrams for (6).

The first two cases ($a < 0$) exemplified in Fig. 1a and Fig. 1b, correspond to unstable behavior according to the Nyquist criterion. Therefore, the stability region in the (a, b) parameter plane may only belong to the right half-plane $a > 0$. The last two cases, however, may correspond to either unstable behavior, as in Fig. 1c and Fig. 1d, or stable behavior, as in Fig. 1e and Fig. 1f.

By taking into account that $|G(j\omega)|$ decreases monotonically as ω increases (which would not be true in the case of PID controllers), the positive Nyquist diagram intersects the unit circle at one point only. For all values of τ, the stability boundary is formed by a segment of the b-axis ($a = 0$) and by the curve of the (a, b)-plane characterized by:

$$\arg[G(j\omega_A)] = -\pi, \tag{14}$$

along which $m_\phi = 0$. (Note that, if $\arg[G(j\omega_A)] = -(2k+1)\pi$, $k \in Z_+$, the system would not be stable because the Nyquist diagram would encircle the critical point).

The curves corresponding to phase margins greater than zero are included in the just-defined stability region. The stability boundaries for various values of τ are depicted in Fig. 2, whereas the curves corresponding to a set of values of m_ϕ for the same value of τ ($\tau = 0.5$) are shown in Fig. 3. These have been obtained with a MATLAB program that repeatedly solves equations (11a) and (11b).

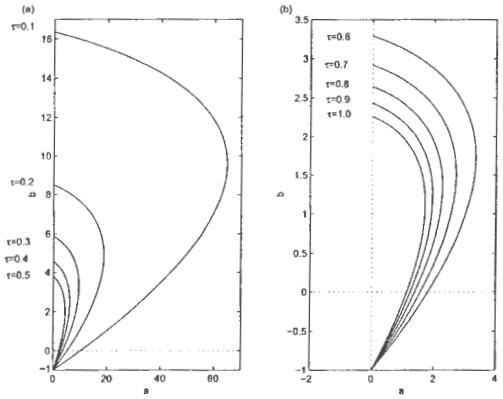

Fig. 2. Stability regions of the (a, b)-plane: (a) $\tau = 0.1 \div 0.5$; (b) $\tau = 0.6 \div 1.0$.

V. GAIN CROSS-OVER FREQUENCY

The analytic expression of the curves on the (a, b)-plane corresponding to $\omega_A = const$ can immediately be determined from the condition $|G(j\omega_A)| = 1$. In fact, taking account of (6) and considering square magnitudes, we get:

$$\frac{a^2 + b^2\omega_A^2}{\omega_A^2(1+\omega_A^2)} = 1 \tag{15}$$

and then:

$$a^2 + \omega_A^2 b^2 - \omega_A^2 - \omega_A^4 = 0 \tag{16}$$

which represents an ellipse centered at $(a = 0, b = 0)$ whose axes belong to the straight lines $a = 0$ and $b = 0$. These ellipses intersect the vertical axis for $a = 0$ and

$$b = \pm\sqrt{1+\omega_A^2}, \tag{17}$$

whereas they intersect the horizontal axis for $b = 0$ and

$$a = \pm\omega_A\sqrt{1+\omega_A^2}. \tag{18}$$

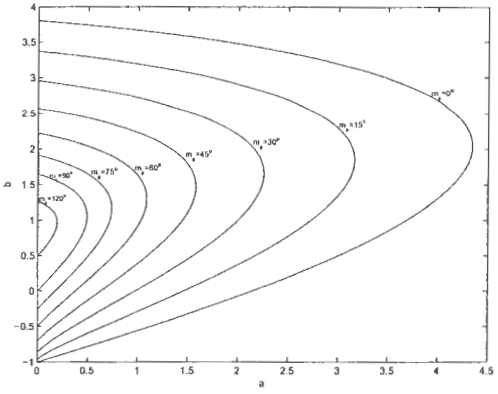

Fig. 3. Curves $m_\phi = const$ in the (a, b)-plane for $\tau = 0.5$.

In particular, for $\omega_A = 1$ the ellipse becomes a circle of radius $\sqrt{2}$; for $\omega_A < 1$ the horizontal axis is smaller than the vertical one, and vice versa for $\omega_A > 1$. It is interesting to observe that the ellipse corresponding to every ω_A intersects the line $b = a$ for $b = a = \omega_A$.

Note, also, that ellipses (16) are independent of τ (whereas the curves $m_\phi = const$ depend on it) and that only their right halves may belong to the stability region. Fig. 4 shows the right halves of the ellipses corresponding to different values of ω_A in the region of interest.

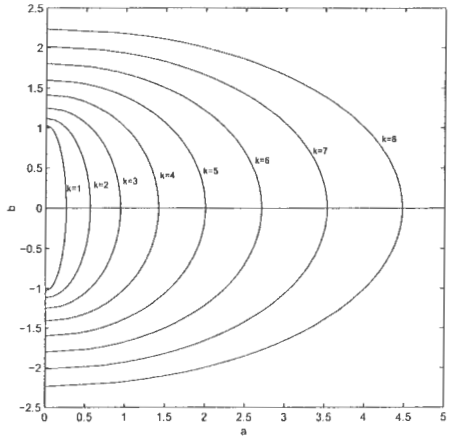

Fig. 4. Arcs of the curves $\omega_A = 0.25k$, $k = 1 \div 8$.

VI. SPECIFICATIONS COMPATIBILITY

According to the considerations of Section I, let us assume that the specifications are expressed as:

$$m_\phi \geq m_\phi^\star, \tag{19}$$

$$\omega_A = \omega_A^\star. \tag{20}$$

Given the process to be controlled, and thus τ, specifications (19) and (20) are compatible with each other if, on the parameter plane corresponding to such τ, an arc of the ellipse $\omega_A = \omega_A^\star$ belongs to the region between the curve $m_\phi = m_\phi^\star$ and the vertical axis. For instance, for $\tau = 0.5$ the condition $\omega_A = 2$ is not compatible with $m_\phi \geq 75°$, whereas it is compatible with $m_\phi \geq 45°$; in fact, as shown in Fig. 5, the curve $\omega_A = 2$ is external to the curve $m_\phi = 75°$, whereas it intersects the curve $m_\phi = 45°$ at point P_1 so that the points of arc P_1P_2 exhibit a phase margin greater than 45° (precisely, it ranges from 45° to almost 60°).

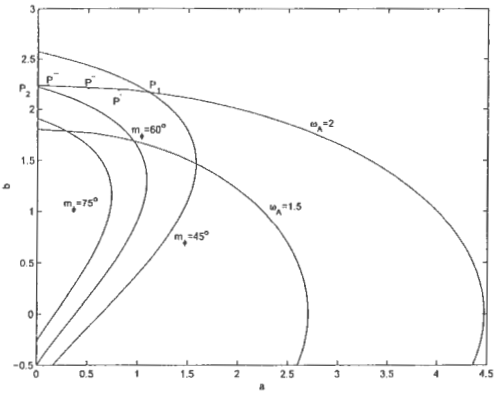

Fig. 5. Compatibility of conditions $\omega_A^\star = 2$ and $\omega_A^\star = 1.5$ with $m_\phi \geq 75°$, $m_\phi \geq 60°$ and $m_\phi \geq 45°$ for $\tau = 0.5$.

On the other hand, it is easy to find analytically the highest value m_ϕ^u of m_ϕ compatible with a cross-over frequency ω_A. In fact, m_ϕ^u characterizes the curve of constant m_ϕ intersecting the ellipse for such ω_A at $a = 0$ (upper intersection of the ellipse with the vertical axis). Now, when $a = 0$, the phase of the open-loop frequency response $G(j\omega)$ is $\arg[G(j\omega)] = -\tau\omega - \arctan(\omega)$, so that the phase margin turns out to be:

$$m_\phi = m_\phi^u = \pi - \tau\omega_A - \arctan(\omega_A). \tag{21}$$

It follows that the specified phase margin $m_\phi^\star$ is compatible with $\omega_A^\star$ if:

$$m_\phi^\star < \pi - \tau\omega_A^\star - \arctan(\omega_A^\star). \tag{22}$$

For example, if $\omega_A^\star = 2$ and $\tau = 0.5$, then $m_\phi^u < 1.034$ rad $= 59.27°$. Fig. 6 plots the value of m_ϕ^u (in rad) vs. ω_A (in rad/s) for some values of τ.

VII. DESIGN CHARTS AND ROBUSTNESS ANALYSIS

The design procedure can be illustrated by referring to charts depicting the loci $m_\phi = const$ and $\omega_A = const$ in the region of interest of the (a, b)-plane for different values of τ. Charts of this kind are shown in Fig. 7.

The design procedure can be stated as follows:

(i) refer to the chart corresponding to the value of $\tau = \frac{L}{T}$ equal (or closest) to the actual normalized delay;

(ii) check whether specifications (19) and (20) are compatible (if they are not so, either modify the normalized gain cross-over frequency $\omega_A^\star$ or resort to a more complicated controller);

(iii) determine (if necessary, by interpolation) the coordinates (a, b) of a point P on the curve $\omega_A = \omega_A^\star$ included between its intersections with the curve $m_\phi = m_\phi^\star$ and the vertical axis, like points P', P'' and P''' in Fig. 5 (the choice of P is discussed in Section IX);

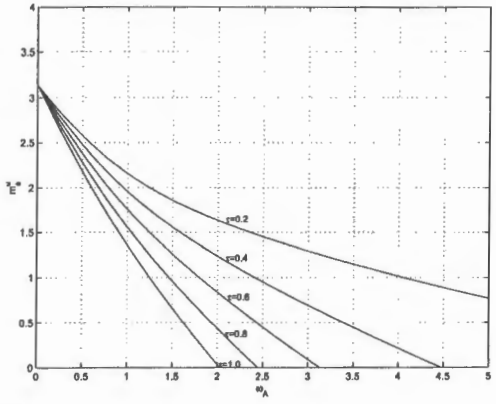

Fig. 6. Highest value m_ϕ^* of the phase margin vs. cross-over frequency ω_A for $\tau = 0.2, 0.4, 0.6, 0.8, 1.0$.

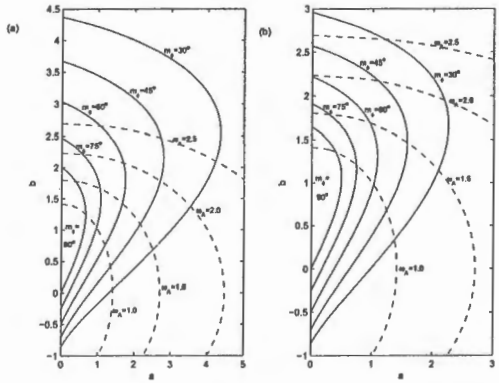

Fig. 7. Loci $m_\phi = const$ (solid lines) and $\omega_A = const$ (dashed lines) in the (a, b)-plane: (a) $\tau = 0.3$; (b) $\tau = 0.5$.

(iv) using relations (7a), (7b) and (7c) compute the controller parameters as:

$$K_P = \frac{b}{K}, \qquad K_I = \frac{a}{KT} \qquad \text{or} \qquad T_I = \frac{bT}{a}. \tag{23}$$

The above charts can also be used to evaluate the effects on m_ϕ and $\hat{\omega}_A$ of changes in the process parameters.

To this purpose, let us denote by K_P and K_I the values of the controller parameters ensuring that $m_\phi = \bar{m}_\phi \leq m_\phi^*$ and $\hat{\omega}_A = \hat{\omega}_A^*$ when the process parameters take the "nominal" values K, L and T, and denote K', L' and T' their modified values. By keeping the controller unchanged, the new process parameters lead to the following values for the parameters of the normalized loop transfer function:

$$a' = K' K_I T', \qquad b' = K' K_P, \qquad \tau' = \frac{L'}{T'}. \tag{24}$$

Using the chart for τ', the new phase margin m'_ϕ and normalized cross-over frequency ω'_A corresponding to (a', b') can be evaluated, from which the new actual cross-over frequency $\hat{\omega}'_A = \frac{\omega'_A}{T'}$ is immediately obtained.

To measure the effects of the considered process modification, it is reasonable to consider the deviations Δm_ϕ and $\Delta\hat{\omega}_A$ of the new values $m_\phi^{'}$ and $\hat{\omega}_A^{'}$ from the old values $\bar{m}_\phi$ and $\hat{\omega}_A^*$ of phase margin and cross-over frequency, i.e.:

$$\Delta m_\phi := m_\phi^{'} - \bar{m}'_\phi, \tag{25}$$

$$\Delta\hat{\omega}_A := \hat{\omega}_A^{'} - \hat{\omega}_A^*. \tag{26}$$

In practice, it will only be possible to predict the ranges $[K_m, K_M]$, $[L_m, L_M]$, $[T_m, T_M]$ over which the process parameters K, L, T, respectively, can vary. These intervals define a parallelepiped of the original process parameter space that is mapped via relations (7a), (7b), (7c), with K_P and K_I constant, into a 6-face solid of the (a, b, τ) space characterized by $2^3 = 8$ vertices and 12 edges. To facilitate the determination of the worst case, a MATLAB program has been developed to represent the cross sections of this solid on the charts for a suitable number of τ values in the interval of interest, i.e., $\tau \in [\frac{L_m}{T_M}, \frac{L_M}{T_m}]$.

As far as m_ϕ is concerned, the worst case usually corresponds to either the vertex $[K_M, L_M, T_m]$ or to the vertex $[K_M, L_M, T_M]$.

As far as the cross-over frequency is concerned, simple analytical considerations (equations (15) and (16)) show that its largest value is achieved for K_M and T_M and its smallest value for K_m and T_m.

VIII. GAIN MARGIN

The Nyquist diagram of the loop function (6) crosses the negative real axis an infinite number of times. The value of ω_B of the frequency ω corresponding to the first intersection is the so-called phase cross-over frequency. Denoting by g the absolute value of (6) at this point, we have:

$$G(j\omega_B) = -g. \tag{27}$$

As is known, the gain margin m_g can be defined in different ways, e.g., $m_g = 1 - g$ or $m_g = \frac{1}{g}$ or, especially with reference to Bode diagrams, $m_g = \log\frac{1}{g} = -\log g$. To simplify the analysis we directly refer to g, from which the gain margin may be obtained immediately, whatever definition is adopted.

Multiplying both sides of (27) by $j\omega_B - \omega_B^2$ and equating real and imaginary parts, we get:

$$a = g\,\omega_B[\sin(\tau\omega_B) + \omega_B\cos(\tau\omega_B)], \tag{28a}$$

$$b = g[\omega_B\sin(\tau\omega_B) - \cos(\tau\omega_B)]. \tag{28b}$$

Given τ, for any value of g equations (28a) and (28b) define a curve in the (a, b)-plane with current coordinate ω_B. Of course, the curve for $g = 1$ coincides with the curve characterized by $m_\phi = 0°$ of the family previously considered, and forms the boundary of the stability region together with the relevant segment of the b-axis. Inside the stability region, the curves $g = const$ $(0 < g < 1)$ have the shape shown in Fig. 8. Their shape is roughly similar to that of curves $m_\phi = const$ (cf. Fig. 7). However, the two intersections of every $g = const$ with the vertical axis always include point $(0, 0)$, whereas the two intersections of every curve $m_\phi = const$ always include point $(0, 1)$.

Concerning the curves $\omega_B = const$ (which determine the parametrization of those for $g = const$), their analytical expression, easily obtained from equations (28a) and (28b), is simply:

$$b = pa \tag{29}$$

which represents a straight line through the origin whose angular coefficient:

$$p = \frac{\omega_B\sin(\tau\omega_B) - \cos(\tau\omega_B)}{\omega_B[\sin(\tau\omega_B) + \omega_B\cos(\tau\omega_B)]} \tag{30}$$

is independent of g (but depends on τ). The lines $\omega_B = const$ are also drawn in Fig. 8.

The charts in Fig. 8 allow us to find the gain margin (and the related phase cross-over frequency ω_B) associated with a pair (a, b) determined according to the design procedure of Section V, i.e., satisfying the specifications on m_ϕ and ω_A, and can thus be used to discriminate the points of the "admissible" arc of the parameter plane (like arc P_1P_2 of Fig. 5): note in this regard, that a not too small value of g is often preferable (see later).

Clearly, if the design is based on m_ϕ and m_g, instead of m_ϕ and ω_A, it is useful to avail ourselves of charts depicting, for every τ, the curves $m_\phi = const$ and $g = const$ inside the stability region. In this case, by denoting with m_ϕ^* and g^* the specified lower bound on m_ϕ and upper bound on g, the specifications are compatible if curve $m_\phi = m_\phi^*$ crosses curve $g = g^*$ on the chart for the relevant value of τ, and the acceptable values of the normalized controller parameters will

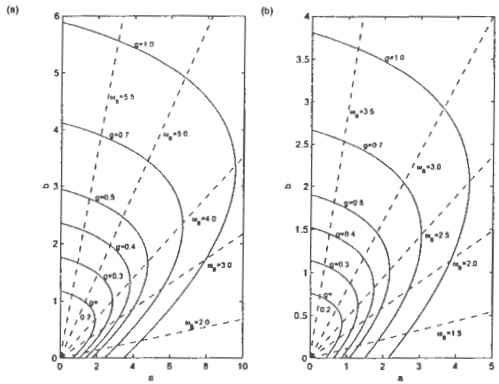

Fig. 8. Curves $g = const$ (solid lines) and lines $\omega_B = const$ (dashed lines) in the (a, b)-plane: (a) $\tau = 0.3$; (b) $\tau = 0.5$.

correspond to the points in the intersection of the regions where $m_\phi \geq m_\phi^*$ and $g \leq g^*$. The procedure is exemplified in Fig. 9 with reference to $\tau = 0.5$, $m_\phi^* = 60^o$ and $g^* = 0.3$: curves $m_\phi = 60^o$ and $g = 0.3$ intersect each other at $(1, 0.916)$ for $\omega_A = 0.96$ and at $(0.221, -0.200)$ for $\omega_A = 0.21$. The Nyquist diagrams of the loop functions corresponding to these two points practically coincide, except for their graduation in ω, along the arc between the intersection with the real axis, and slightly differ outside this arc. Correspondingly, the overshoots of the step responses of the two feedback systems are about the same, whereas the ratio between their rise times is almost reciprocal to the ratio between the related gain cross-over frequencies.

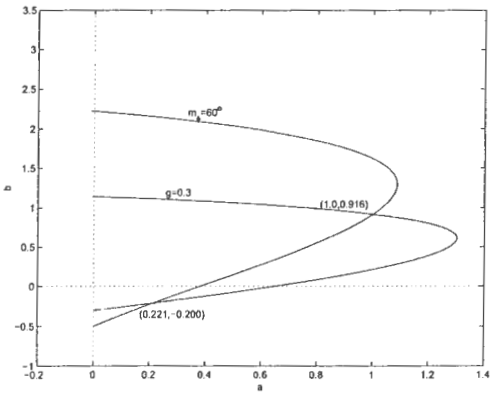

Fig. 9. Regions where $m_\phi \geq 60^o$ and $g \leq 0.3$ for $\tau = 0.5$.

IX. CHOICE OF A POINT (a, b) IN THE ADMISSIBLE REGION

If the specifications are compatible, they can be satisfied in different ways. The following considerations help us identify the solutions that are most satisfactory for the specific problem at hand.

As already said, if the specifications are given in terms of gain cross-over frequency and phase margin, i.e., in the form $\omega = \omega_A^*$ and $m_\phi \geq m_\phi^*$, the admissible region of the (a, b)-plane reduces to the arc of the ellipse $\omega_A = \omega_A^*$ between its intersections with the curve $m_\phi = m_\phi^*$ and the b-axis, like arc P_1P_2 of Fig. 5 which refers to the case of $\tau = 0.5$,

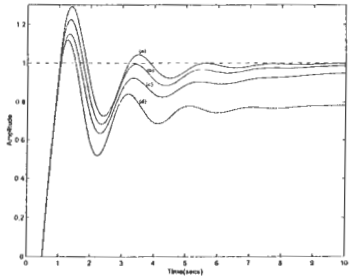

Fig. 10. Step responses of the feedback control system for $\tau = 0.5$, $\omega_A = \omega_A^* = 2$ and $m_\phi \geq m_\phi^* = 45^o$: (a) $a = 1.1023$, $b = 2.1671$ ($m_\phi = 45^o$); (b) $a = 0.8$, $b = 2.2$ ($m_\phi \approx 49^o$); (c) $a = 0.5$, $b = 2.2$ ($m_\phi \approx 53^o$); (d) $a = 0.1$, $b = 2.2355$ ($m_\phi \approx 58^o$).

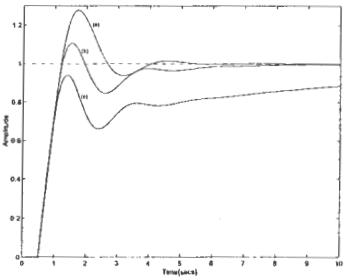

Fig. 11. Step responses for $\tau = 0.5$, $\omega_A = 1.5$ and: (a) $m_\phi = 45^o$ ($a = 1.5786$, $b = 1.4637$); (b) $m_\phi \approx 60^o$ ($a = 0.9566$, $b = 1.686$); (c) $m_\phi \approx 75^o$ ($a = 0.2842$, $b = 1.7859$).

$\omega_A^* = 2$ and $m_\phi^* = 45^o$. It is instructive to examine the step response of the feedback control system corresponding to different points of arc P_1P_2. To this purpose, Fig. 10 shows the responses for:

(i) point $P_1 = (1.1023, 2.1671)$, where $m_\phi = 45^o$;

(ii) point $P' = (0.8, 2.2)$, where $m_\phi \simeq 49^o$;

(iii) point $P'' = (0.5, 2.\bar{2})$, where $m_\phi \simeq 53^o$;

(iv) point $P''' = (0.1, 2.2355)$, very close to P_2, where $m_\phi \simeq 58^o$.

For $t > \tau$, all responses are well approximated by the step response of a third-order system with two complex poles. On passing from P_1 to P_2, the importance of the aperiodic mode increases. As a result, the time to reach half the final value and the rise time remain (practically) unchanged, whereas the overshoot, strictly related to the phase margin, decreases and the settling time increases.

Similar conclusions can be drawn with reference to the step responses represented in Fig. 11, which correspond to the intersections of the ellipse $\omega_A = 1.5$ with the curves $m_\phi = 45^o$, $m_\phi = 60^o$ and $m_\phi = 75^o$, also shown in Fig. 5. The last two intersections, like the points on the arc P_1P_2 considered in Fig. 10, lie above the line $b = a$, along which, as already observed in Section 3, the gain cross-over frequency is $\omega_A = a = b$. The first intersection, in contrast, is below this line, but quite close to it. Now, for $a = b$ the zero introduced by the controller cancels the pole at -1 of the normalized process and the feedback system exhibits only two dominant poles (this can easily be explained with the aid of root locus considerations; its part closest to the origin contains arcs of two branches only). For this reason, for $t > \tau$ the step response corresponding to $\omega_A = 1.5$ and $m_\phi = 45^o$ (curve (a) of Fig. 11) is very similar to that of a second-order system, whereas the other responses are characterized by three dominant poles (the poles closest to the origin) and, therefore, contain an additional aperiodic mode.

Concerning the choice of a point in the admissible region when the specifications are in terms of phase and gain margins, let us consider again the example illustrated in Fig. 9. The point $(1, 0.916)$ at the intersection of the curves $m_\phi = m_\phi^* = 60^o$ and $g = g^* = 0.3$ is very close to the straight line $b = a$. The step response of the related feedback control system is represented in Fig. 12 together with the responses for $a = b = 0.75$ (where the settling time is almost minimal) and $a = b = 0.5$ corresponding to points inside the admisible region. For the reasons previously explained, all these responses are very similar to second-order responses (for $t > \tau$). As the considered point approaches the origin along the above-mentioned straight line $a = b$, m_ϕ increases (from 60^o to 75.7^o) and ω_A decreases (from 0.96 to 0.5). Correspondingly, the responses become monotonically increasing with longer rise times. If, instead, the (a, b)-point approaches the b-axis along the horizontal line $b = 0.916$), the step responses change as shown in Fig. 13: the importance of the additional (aperiodic) dominant mode increases and the settling time becomes longer.

X. CONCLUSIONS

A simple procedure has been suggested that allows us to check the compatibility of the specifications with the use of PI controllers and facilitate the determination of their parameters. On the basis of linear interpolation equations (11), MATLAB programs have been developed for finding the loci of constant stability margins and cross-over frequencies in the parameter space of a suitably normalized open-loop transfer function. In this way, the effects of process changes on system performance can easily be evaluated. Finally, with the aid of representative examples, criteria have been suggested to guide the choice of a design solution among the admissible ones.

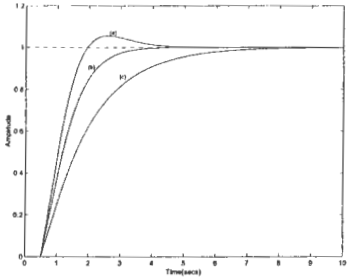

Fig. 12. Step responses for $\tau = 0.5$ corresponding to points on, or close to, the line $b = a$: (a) $a = 1.0$, $b = 0.916$ ($m_\phi = 60^o$, $g = 0.3$, $\omega_A = 0.96$); (b) $a = b = \omega_A = 0.75$ ($m_\phi = 68.5^o$, $g = 0.24$); (c) $a = b = \omega_A = 0.5$ ($m_\phi = 75.7^o$, $g = 0.16$).

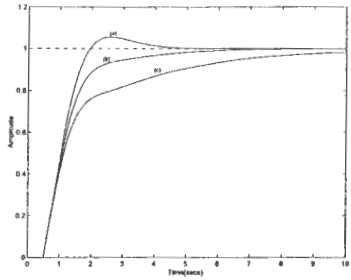

Fig. 13. Step responses for $\tau = 0.5$ corresponding to points on the horizontal line $b = 0.916$: (a) $a = 1.0$ ($m_\phi = 60^o$, $g = 0.3$, $\omega_A = 0.96$); (b) $a = 0.75$ ($m_\phi = 72.2^o$, $g = 0.28$, $\omega_A = 0.82$); (c) $a = 0.5$ ($m_\phi = 88.3^o$, $g = 0.26$ $\omega_A = 0.65$).

References

[1] K. J. Åström and T. Hägglund, *PID Controllers: Theory, Design, and Tuning*. 2nd ed. Research Triangle Park, NC: Instrument Society of America, 1995.

[2] W. L. Bialkowski, "Dreams versus reality: a view from both sides of the gap," *Pulp and Paper Canada*, Vol. 94, No. 11, 1993.

[3] D. B. Ender, "Process control performance: not as good as you think," *Control Engineering*, Vol. 40, No. 10, pp. 180-190, 1993.

[4] A. O'Dwyer, "Time delayed process model parameter estimation: A classification of techniques" in *Proc. Int. Conf. Control 2000*, Cambridge, England, 2000.

[5] J. G. Ziegler, N. B. Nichols. "Optimum settings for automatic controllers," *Trans. ASME*, Vol. 64, pp. 759-768, 1942.

[6] W. K. Ho, T. H. Lee, H. P. Han, and Y. Hong, "Self-tuning IMC-PID control with interval gain and phase margins assignment," *IEEE Trans. Contr. Syst. Technol.*, Vol. 9, pp. 535-541, 2001.

[7] D. Vrancic, S. Strmsnik, and D. Juricic, "A magnitude optimum multiple integration tuning method for filtered PID controller," *Automatica*, Vol. 37, pp. 1473-1479, 2001.

[8] G. J. Silva, A. Datta, and S. P. Bhattacharyya, "PI stabilization of first-order systems with time delay," *Automatica*, Vol. 37, pp. 2025-2031, 2001.

[9] "Special Section on PID Control," *IEE Proc. Control Theory Appl.*, Jan. 2001.

[10] G. J. Silva, A. Datta, and S. P. Bhattacharyya, "New results on the synthesis of PID controllers," *IEEE Trans. Automat. Contr.*, Vol. 47, pp. 241-252, 2002.

[11] W. K. Ho, K. W. Lim, C. C. Hang, and L. Y. Ni, "Getting more phase margin and performance out of PID controllers," *Automatica*, Vol. 35, pp. 1579-1585, 1999.